Thin Solid Films 552 (2014) 18–23

Contents lists available at ScienceDirect

Thin Solid Films

journal homepage: www.elsevier.com/locate/tsf

Crystallization mechanism of silicon quantum dots upon thermal annealing of hydrogenated amorphous Si-rich silicon carbide films

Guozhi Wen [a,b], Xiangbin Zeng [a,*], Wugang Liao [a], Chenchen Cao [a]

[a] *School of Optical and Electronic Information, Huazhong University of Science and Technology, Wuhan, Hubei 430074, China*
[b] *School of Electronic and Electrical Engineering, Wuhan Polytechnic University, Wuhan, Hubei 430023, China*

ARTICLE INFO

Article history:
Received 28 December 2012
Received in revised form 25 November 2013
Accepted 2 December 2013
Available online 8 December 2013

Keywords:
Silicon
Silicon carbide
Quantum Dots
Bonding Configuration
Crystallization Mechanism
Plasma-Enhanced Chemical Vapor Deposition
Transmission Electron Microscopy

ABSTRACT

We have investigated the crystallization process of silicon quantum dots (QDs) imbedded in hydrogenated amorphous Si-rich silicon carbide (a-SiC:H) films. Analysis reveals that crystallization of silicon QDs upon thermal annealing of the samples can be explained in terms of bonding configuration and evolution of microstructure. The precursor gases were dissociated via electron impact reactions in the plasma-enhanced chemical vapor deposition, where the hydrogenated silicon radicals and reactive SiH_n species lead to the formation of primary Si nuclei. With increasing annealing temperature, the breaking of SiH_n bonds and decomposition of Si-rich SiC were progressively enhanced, allowing the formation of crystalline silicon QDs inside the a-SiC:H matrix. The results help clarify a probable mechanism for the growth of silicon QDs and provide the possibility to optimize the microstructure of silicon QDs in a-SiC:H films.

© 2013 Elsevier B.V. All rights reserved.

1. Introduction

As an unlimited and pollution-free energy source device, solar cells have been paid much attention recently. However, the reported efficiencies of conventional Si solar cells are lower than the ideal values [1–3]. The power-generating costs are, in this way, higher than that of thermal power generation systems or hydroelectric systems. To circumvent the Shockley–Queisser limit, multiple energy threshold approaches, such as all-silicon tandem cells using silicon QDs, are proposed [4,5]. There is a unique quantum size effect in QDs [6], which reveals that the bandgap of QDs can be properly tuned, depending on the dot dimension distribution. For all-silicon tandem solar cells using silicon QDs, the higher-energy photons can be absorbed at higher bandgaps, while the lower-energy photons can be absorbed at the lower bandgaps. Thus silicon QDs, especially those with diameters less than the Bohr radius of exciton (~5 nm) in amorphous dielectric semiconductors, have been a subject of intensive research efforts [7–9].

Present efforts on silicon QDs are mainly allocated in preparation of silicon QDs embedded in a variety of semiconductor materials, such as non-stoichiometric silicon-oxide (SiO_x), silicon-nitride (SiN_x) and silicon-carbide (SiC_x). The tunneling barrier for electrons and holes between adjacent silicon QDs in amorphous SiC_x (2.5 eV) is lower than that in SiO_x (9.0 eV) or SiN_x (5.3 eV), where carriers can be easily transported and greater tunneling currents can be expected [5]. Amorphous Si-rich SiC films comprising silicon QDs are considered to be good candidates for the fabrication of future third generation Si-based photovoltaic devices [10].

Several different preparation techniques of silicon QDs in amorphous SiC matrix are under development. Considerable reports have been published about the formation of silicon QDs, as well as about exploration of their microstructure, photoluminescence and electrical properties [11]. In spite of the importance and availability of these materials, the key points for a full understanding about the structural evolution or crystallization process of silicon QDs upon thermal annealing of Si-rich a-SiC:H films have been less documented, and the discussion is still open [12–14].

2. Experimental details

Non-stoichiometric a-SiC:H samples were fabricated by decomposition of H_2-diluted 10% silane (SiH_4) and pure methane (CH_4) gas mixtures on (100) crystal silicon wafers and quartz (SiO_2) plates simultaneously. The radio frequency of the plasma-enhanced chemical vapor deposition (PECVD) system was 13.56 MHz. The vacuum chamber had a base pressure of less than 2.0×10^{-4} Pa. Deposition was carried out at a working pressure of 106.7 Pa. The power density and the growth temperature were fixed at 160 $mW \cdot cm^{-2}$ and 200 °C, respectively. The flow rate of SiH_4 was maintained at 50 sccm and CH_4 at 30 sccm. After deposition, the samples were cut into smaller parts.

To explore the crystallization or growth process of silicon QDs in the SiC host matrix, each part was annealed subsequently in a quartz tube

* Corresponding author. Tel./fax: +86 27 87544760.
E-mail address: eexbzeng@mail.hust.edu.cn (X. Zeng).

0040-6090/$ – see front matter © 2013 Elsevier B.V. All rights reserved.
http://dx.doi.org/10.1016/j.tsf.2013.12.001

furnace with a 99.999% N_2 atmosphere for 30 min at different temperatures. The chemical bonding configuration behaviors were deduced from Fourier transform infrared absorption measurements (FTIR, VERTEX 70). The chemical composition analyses were carried out with X-ray photoelectron spectroscopy (XPS, VG MultiLab 2000), using a monochromatic Al Kα (1486.5 eV) X-ray source and a hemispherical energy analyzer. The X-ray source power was 300 W. The instrument resolution was 0.47 eV. The working pressure was below 6.67×10^{-8} Pa. The analyzed area of the sample was about 0.36 mm^2. Before detections, the samples were sputtered using a beam of 3 kV × 2 μA Ar^+ bombardments for 180 s. The spectra were collected at 25 eV pass energy and the narrow-scan peaks were fitted with Thermo Avantage software. The binding energy values were calibrated using the contaminant carbon $C_{1s} = 284.6$ eV. A standard Smart background was used for fitting the spectra.

The crystalline phase and crystallinity were characterized by Raman scattering (HORIBA Jobin Yvon LabRAM Spectrometer HR 800 UV) in backscattering configuration. The laser light came from an Ar^+ ion laser with a wavelength of 514.5 nm. The crystalline phase was further characterized by grazing incidence X-ray diffraction, using a Philips X'Pert Pro (XRD, PANalytical PW3040/60) at a voltage of 40 kV and a current of 40 mA, with Cu Kα radiation (λ = 1.540562 Å). The glancing angle between the incident X-ray and sample surface was 1.0°. A semi-quantitative analysis of QD size was performed by X'Pert HighScore software. The direct observations of the microstructure were performed by transmission electron microscopy (TEM, JEM-2100F) and selected area electron diffraction (SAED, JEM-2010 HT) operated at 200 kV. The specimen for TEM and SAED analyses was reduced down to some tens of nanometers by a standard mechanical thinning technique and subsequent Ar^+ ion milling polishing.

3. Results and discussion

Direct physical evidence of the formation of silicon QDs in the non-stoichiometric a-SiC:H samples was displayed by a high resolution TEM. Fig. 1(a) shows a representative plan-view image of the sample annealed at 1050 °C, where a high density of isolated black spots could be identified, as well as coalescence of parts of the adjacent spots in a homogenous host matrix. Fig. 1(b) depicts the high resolution image of one perfect crystalline QD, where the lattice fringes could be observed clearly. The lattice spacing measured equals to approximately 3.17 Å. Fig. 1(c) displays the SAED pattern, where there are three diffraction rings and obvious diffuse aureoles. The diffraction rings reveal that the structure is polymorphous for the 1050 °C annealed non-stoichiometric SiC sample [15]. Radii of the rings are 3.12, 2.11 and 1.64 nm, respectively, which match well with the lattice parameters of the (111), (220) and (311) planes of c-Si [16]. Therefore, the black spots could be attributed to crystalline silicon QDs. The uniformity of the diffraction rings reveal that the number density of crystallized silicon QDs is very large, the size is very small and the orientations are random in the sample. The diffuse aureoles in vicinity of the 3.12 and 2.11 nm rings could be assigned to the presence of a large amount of amorphous silicon nanoclusters, whose average size is smaller than that of crystalline silicon QDs. At the same time, there are faint rings around 2.77 nm and several feeble bright spots dispersed in a circle with a radius of about 2.53 nm in the pattern, which could be ascribed to the amorphous carbon and crystalline SiC nanoparticles, respectively [17]. These feeble spots and faint rings reveal that only a small portion of crystalline SiC or carbon particles exist in the sample [18].

In order to investigate the crystallization process of silicon QDs, chemical bonding configuration behaviors of the as-grown samples and the samples annealed at temperatures of 750, 900, 1050 and 1200 °C were characterized by infrared absorption spectrometry. The absorption of substrate was eliminated by a bare silicon wafer. As Fig. 2 shows, two prominent absorption bands are observed for the as-grown sample. The prominent band around 2085 cm^{-1} could be assigned to SiH_n (n = 1,2,3) and/or C–SiH stretching vibration mode [19]. The other prominent band extending from 500 to 1200 cm^{-1} could be ascribed to superposition of the following four absorption components: SiH_n (n = 1,2,3) rocking and wagging mode near 655 cm^{-1} [20], Si–C non-hydrogen rocking and/or wagging mode or Si–CH_3 stretching vibration mode near 780 cm^{-1} [21], SiH_2 bending vibration mode at 800–900 cm^{-1} [22], CH_n (n = 1,2,3) wagging or bending vibration mode near 1000 cm^{-1} [23].

When the annealing temperature is elevated from ambient circumstance to 750 °C, the SiH_n and/or C–SiH mode around 2085 cm^{-1} disappear completely, the SiH_n mode near 655 cm^{-1} and CH_n near 1000 cm^{-1} diminish and the Si–C or Si–CH_3 mode near 780 cm^{-1} increases gradually. When the annealing temperature is further elevated to 1050 °C, the Si–C or Si–CH_3 peak near 780 cm^{-1} is shifted toward

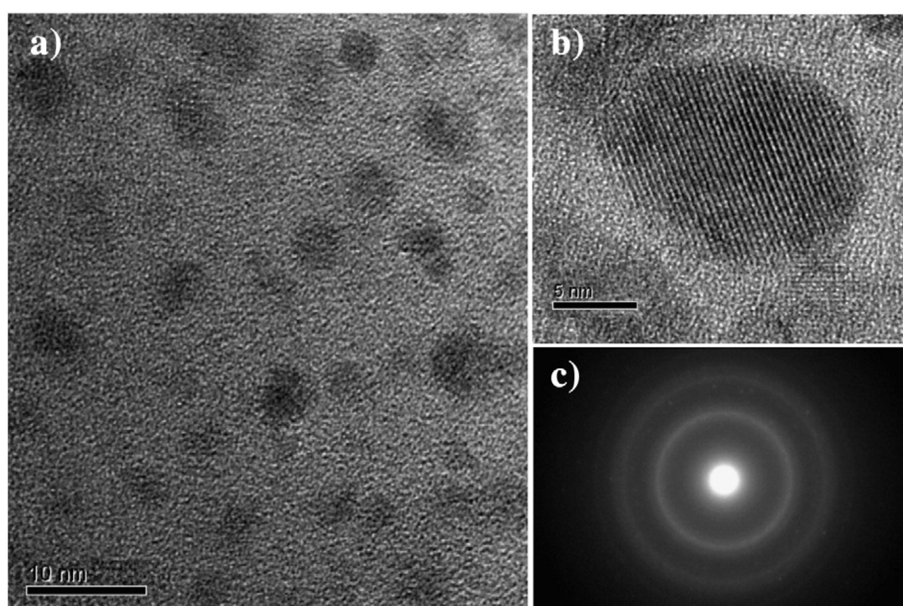

Fig. 1. (a) Typical plan-view high resolution TEM image of the amorphous non-stoichiometric SiC:H sample annealed at 1050 °C, (b) Image of one individual perfect crystalline silicon QD, and (c) Pattern of SAED.

Download English Version:

https://daneshyari.com/en/article/1665678

Download Persian Version:

https://daneshyari.com/article/1665678

Daneshyari.com